on the scalar field are quantitatively similar. This indicates that outside the region where the blockage effect is significant, the passive scalar is unaffected by the strain regardless of the magnitude and direction of the strain.

For $L_0/D = 0.32$ near the stagnation point, vortex stretching causes an increase in the magnitude of the turbulent axial heat flux. At the station nearest to the stagnation point, the distorted axial heat flux is 1.8 times its undistorted value at the same location and experimental conditions. Due to the blockage effect, the axial heat flux for $L_0/D = 3.5$ at the nearest station to the stagnation point is about 40% less than its undistorted value. The variation in the axial heat flux for axisymmetric objects for different L_0/D ratios is qualitatively similar to the corresponding results for the two-dimensional objects. However, since the effect of distortion is less than that for the two-dimensional objects, the amount of attenuation and amplification in the normalized heat flux is less and occurs closer to the stagnation point than for the two-dimensional objects.

Figures 2a–c show the variation of the same quantities as given in Fig. 2 along a line parallel to the edge of the objects ($y = D/2$). The increase and decrease in these quantities are similar but less than the corresponding quantities along the mean stagnation streamline.

References

[1]Hunt, J. C. R., "A Theory of Two-Dimensional Flow Round Two-Dimensional Bluff Bodies," *Journal of Fluid Mechanics*, Vol. 61, Pt. 4, Dec. 1973, pp. 625–706.

[2]Bearman, P. W., "Some Measurement of Distortion of Turbulence Approaching a Two-Dimensional Bluff Body," *Journal of Fluid Mechanics*, Vol. 53, Pt. 2, June 1972, pp. 451–467.

[3]Britter, R. E., Hunt, J. C. R., and Mumford, J. C., "The Distortion of Turbulence by a Circular Cylinder," *Journal of Fluid Mechanics*, Vol. 92, Pt. 2, May 1979, pp. 269–301.

[4]Rahai, H., and LaRue, J. C., "Effect of Flow Distortion on a Turbulent Scalar Field," *Seventh Symposium on Turbulent Shear Flows*, Stanford, CA, Aug. 1989, pp. 14.3.1–14.3.6.

[5]Wyngaard, J. C., Rockwell, L., and Friehe, C., "Errors in the Measurement of Turbulence Upstream of an Axisymmetric Body," *Journal of Atmosphere and Ocean Technology*, Vol. 5, No. 2, 1985, pp. 605–614.

[6]LaRue, J. C., Deaton, T., and Gibson, C. H., "Measurement of High Frequency Turbulent Temperature," *Review of Scientific Instruments*, Vol. 46, No. 6, 1975, pp. 757–763.

[7]Rahai, H. R., and LaRue, J., "Errors in the Measurements of Turbulent Scalar Upstream of Axisymmetric Objects," AIAA Paper 90-1591, June 1990.

Quantifying Thermal Radiation and Convection Effects During Constant-Heat-Flux Irradiation

Terry J. Hendricks*
University of Texas at Austin, Austin, Texas 78758

Nomenclature

C_p = specific heat, J/kg-K
H = nondimensional thermal convection parameter, $(hT_i)/(\alpha_n I)$
h = thermal convection coefficient, W/m^2-K
I = laser intensity, environmental heat flux, W/cm^2
T_a = ambient temperature, K
T_i = initial temperature, K
T_{max} = maximum temperature before material breakdown, K
t = time, s
t_{max} = maximum exposure time before material breakdown, s
x = depth, m
α_n = total or spectral normal surface absorptivity
β = semi-infinite wall parameter, K/s$^{1/2}$ $- (2\alpha_n I)/(\rho C_p \lambda \pi)^{1/2}$
δ = wall thickness, m
ε = total hemispherical surface emissivity
η = thin wall parameter, K/s $- (\alpha_n I)/(\rho C_p \delta)$
θ_{max} = maximum nondimensional temperature, $(T_{max} - T_1)/T_i$
θ_n = nth-order nondimensional perturbation temperature, $\Delta T_n/T_i$
θ_0 = 0th-order nondimensional temperature, $(T_0 - T_i)/T_i$
κ = thermal diffusivity, m^2/s $- \lambda/(\rho C_p)$
λ = thermal conductivity, W/m-K
ξ = nondimensional depth, $x/(\kappa t)^{1/2}$
ρ = density, kg/m^3
σ = Stephan-Boltzmann constant, W/m^2-K^4
χ = nondimensional thermal radiation parameter, $(\sigma \varepsilon T_i^4)/(\alpha_n I)$
ψ_n = nondimensional time parameter, $(\eta t/T_i)$, $(\beta t^{1/2}/T_i)$

Introduction

MATERIAL survivability during constant-heat-flux irradiation is of increasing importance to many defense and commercial applications. Spacecraft and laser weaponry design are major defense applications concerned with material survivability during high-intensity laser irradiation of both ground-based and space-based systems. Commercial applications where material survivability is important include, inertial confinement fusion (ICF) reactor design, Tokamak fusion reactor design, many types of laser-driven materials processing, and thermal protection system (TPS) design in high-velocity planetary re-entry vehicles.

It is often desirable and necessary to have estimates of thermal reradiation and convection effects on material transient thermal response and survivability characteristics during constant-heat-flux irradiation. Although transient thermal response of irradiated materials can be impacted by thermal reradiation and convection conditions at the material surface, little analytical work includes thermal reradiation and convection effects in a closed-form analytic solution. Several references[1–4] discuss analytic solutions to thin-wall, thick-wall, and semi-infinite wall analysis cases, assuming no thermal radiation and convection from the material surface. Abarbanel,[5] Bartholomeusz,[6] and Chen et al.[7] have investigated analytic treatment of thermal conduction in finite-thickness and semi-infinite cooling solids, but not with the combination of incident irradiation, thermal reradiation, and thermal convection at the surface. Roy et al.,[8] Modest et al.,[9,10] Yuen et al.,[11] and Knight[12] effectively treated such complexities as three-dimensional effects, pulsed and moving beams, in-depth absorbing, emitting, and scattering effects on transient heating, and vaporization using numerical techniques, but neglected thermal reradiation and convection effects. This work presents a rapid, accurate analytic methodology to evaluate first-order thermal reradiation and convection impacts on material survivability before breakdown (i.e., ablation, melting) during constant-heat-flux irradiation.

Many constant-flux thermal response problems can be effectively analyzed, at least to a first approximation, with a one-dimensional thermal analysis. This approach is particularly applicable to situations where lateral thermal conduction

Received April 3, 1992; revision received Aug. 13, 1992; accepted for publication Aug. 14, 1992. Copyright © 1992 by the American Institute of Aeronautics and Astronautics, Inc. All rights reserved.

*Ph.D. Candidate, University Fellow, Department of Mechanical Engineering, Center for Energy Studies, 10100 Burnet Road. Member AIAA.

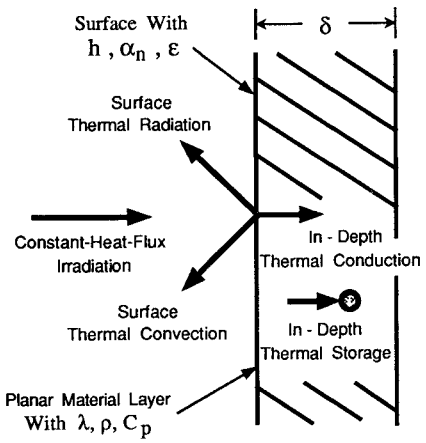

Fig. 1 Uniform laser irradiation to solid surface.

is negligibly small. Figure 1 illustrates the typical one-dimensional thermal model and the pertinent thermal processes considered in this analysis. Ablation, pyrolysis, and phase-change processes are not considered here; these analysis results apply to periods before any kind of material breakdown occurs. In general, h is a function of time as the surface temperature increases, but in this analysis h is considered an "effective" constant value. The radiative absorptivity corresponds to the relevant temperature and irradiation wavelengths. The convection coefficient and thermophysical properties similarly correspond to the appropriate surface/ambient temperatures. This work assumes an adiabatic back surface and an initial temperature equal to the ambient temperature.

Mathematical Formulation

Thin-wall and semi-infinite wall transient response cases represent the important limiting thermal response cases here. Dimensional analysis of the thin-wall case revealed four nondimensional parameters uniquely describing the transient response

$$\theta(t) = \{[T(t) - T_i]/T_i\} = F(\psi_1, \chi, H) \tag{1}$$

and dimensional analysis of the semi-infinite wall problem determined five nondimensional parameters completely describing the transient response

$$\theta(x, t) = \{[T(x, t) - T_i]/T_i\} = G(\psi_2, \chi, H, \xi) \tag{2}$$

$$\psi_1 = \left(\frac{\alpha_n I t}{\rho C_p \delta T_i}\right) \quad \psi_2 = \left(\frac{2\alpha_n I t^{1/2}}{\sqrt{\rho C_p \lambda \pi} T_i}\right) \quad \chi = \left(\frac{\sigma \varepsilon T_i^4}{\alpha_n I}\right)$$

$$H = \left(\frac{h T_i}{\alpha_n I}\right) \quad \xi = \left(\frac{x}{\sqrt{\kappa t}}\right) \tag{3}$$

The mathematical development and solution follows the perturbation and Laplace transform techniques of Hendricks[13] applied to the standard energy-balance differential equations and surface boundary conditions with thermal reradiation and convection included. The thin-wall energy-balance and boundary condition is

$$\rho C_p \delta \frac{\partial T}{\partial t} = \alpha_n I - \sigma\varepsilon(T^4 - T_a^4) - h(T - T_a) \qquad T(t = 0) = T_i \tag{4}$$

Semi-infinite wall energy-balance and boundary conditions are given by

$$\frac{\partial^2 T}{\partial x^2} = \frac{1}{\kappa} \cdot \frac{\partial T}{\partial t}, \qquad T(x, t = 0) = T_i \tag{5}$$

$$-\lambda \left[\frac{\partial T}{\partial x}\right]_{x=0} = \alpha_n T - \sigma\varepsilon[T_{x=0}^4 - T_a^4] - h[T_{x=0} - T_a] \qquad \left[\frac{\partial T}{\partial x}\right]_{x=\infty} = 0 \tag{6}$$

The resulting thin-wall and semi-infinite wall solutions, respectively, are series solutions of basic 0th-order functions and correcting nth-order perturbation functions:

$$\theta(t) = \{[T(t) - T_i]/T_i\} = \theta_0(\psi_1) + \theta_1(\psi_1, \chi, H) + \theta_2(\psi_1, \chi, H) + \ldots \tag{7}$$

$$\theta(x, t) = \{[T(x, t) - T_i]/T_i\} = \theta_0(\psi_2, \xi) + \theta_1(\psi_2, \xi, \chi, H) + \theta_2(\psi_1, \xi, \chi, H) + \ldots \tag{8}$$

The 0th-order nonradiative/nonconvective solutions, $\theta_0(\psi_1)$ and $\theta_0(\psi_2, \xi)$, are respectively

$$\theta_0(\psi_1) = \{[T_0(t) - T_i]/T_i\} = (\eta/T_i)t = \psi_1(t) \tag{9}$$

$$\theta_0(\psi_2, \xi) = \{[T_0(x, t) - T_i]/T_i\} = \psi_2\{\exp[-(\xi^2/4)] + (\sqrt{\pi}/2)\xi \operatorname{erfc}(\xi/2)\} \tag{10}$$

First- and second-order perturbation functions, θ_1 and θ_2, in Eqs. (7) and (8) are complex power series in the nondimensional variables, χ, H, and ψ_1 or ψ_2. Hendricks[13] discusses and illustrates the mathematical form of these perburbation functions in solutions including thermal reradiation effects.

The perturbation/Laplace transform techniques generated rapid, approximate analytic solutions which give accurate results for surface, and in-depth thermal response without the nodalization, computational stability, and high-gradient grid refinement considerations associated with computational techniques often used in these problems. The thin-wall and semi-finite wall thermal response solutions are exact in the limit of small χ and H. They allow very rapid evaluation of first-order thermal reradiation and convection impacts on material transient thermal performance for a broad range of conditions and material properties.

Material Thermal Absorption/Survivability Effects

Rohsenow et al.[3] illustrates that, for negligible surface reradiation and convection, the maximum exposure time t_{max} for any material is related to the surface heat flux, material properties, material thickness, and a material's maximum allowable temperature by the nondimensional relation:

$$\{\alpha_n I \sqrt{t_{max}}/[\sqrt{\rho C_p \lambda}(T_{max} - T_i)]\} = f(\delta/\sqrt{\kappa t_{max}}) \tag{11a}$$

In the thin-wall case, $f = \delta/\sqrt{\kappa t_{max}}$; in the semi-infinite wall case, $f = \sqrt{\pi}/2$; while in the finite-thickness wall, f is a more complex function of $\delta/\sqrt{\kappa t_{max}}$. This work disclosed a material's thermal absorption capability is uniquely described by the same parameters relating the maximum exposure time to surface heat flux, material properties, material thickness, and maximum surface temperature. However, when thermal reradiation and convection are considered, the Eq. (11a) thermal absorption relationship is modified to represent the first-order thermal radiation and convection impacts on material thermal response. More generally

$$\{\alpha_n I \sqrt{t_{max}}/[\sqrt{\rho C_p \lambda}(T_{max} - T_i)]\} = J(\chi, H) \geq f[\delta/\sqrt{\kappa t_{max}}] \tag{11b}$$

Close examination of Eq. (11b) for thin-wall analysis and semi-infinite wall analyses reveals it is a mathematical relation between the nondimensional parameters discussed here

$$[\eta t_{max}/(T_i \theta_{max})] = (\psi_{1,max}/\theta_{max}) = y(\chi, H) \geq 1 \tag{12a}$$

$$[\beta \sqrt{t_{max}}/(T_i \theta_{max})] = (\psi_{2,max}/\theta_{max}) = z(\chi, H) \geq 1 \tag{12b}$$

for the thin-wall and semi-infinite wall cases, respectively. Any material's thermal response capability and maximum exposure time t_{max} to a given heat flux for any thermal reradiation and convection condition is uniquely determined by χ, H, and $\psi_{1,max}$ or $\psi_{2,max}$. Equations (12a) and (12b) are evaluated directly, for any χ and H, from the thin-wall and semi-infinite wall thermal response solutions given in Eqs. (7) and (8) above, and by Hendricks.[13]

Figures 2–4 are representative illustrations of the general thermal absorption capability [Eqs. (12a) and (12b)] of aluminum and beryllium as a function of H and χ. The impact of thermal reradiation and convection on thermal absorption in these materials relative to the nonradiative/nonconvective ($\chi = 0$, $H = 0$) case is clearly demonstrated. The effect and significance of thermal convection on absorption performance is small is all three cases, until H increases to 0.01. Comparing the Figs. 2 and 3 results for aluminum shows that thermal reradiation effects are clearly more significant than convection effects; results for $\chi = 0.001$, $H = 0$ show more impact on absorption performance than results for $\chi = 0.0001$, $H = 0.001$. Figures 2–4 quantify, relative to a nonradiative/nonconvective case, the exposure time enhancement before material breakdown (i.e., ablation, melting) for a given environmental heat flux when thermal reradiation and convection effects are present; both thin-wall and semi-infinite wall results shift toward increased t_{max} when $\chi > 0$ and $H > 0$. Also, given an exposure time, decreased material thicknesses are possible due to thermal reradiation and convection cooling effects; both thin-wall and finite-wall results also shift toward decreased δ when $\chi > 0$ and $H > 0$. The arrows on Figs. 2–4 indicate the general shift of finite-wall absorption behavior (i.e., dashed line) as it necessarily follows the thin-wall and semi-infinite wall absorption behavior shifts; thin wall and semi-infinite wall cases always bounding the finite-thickness thermal absorption performance.

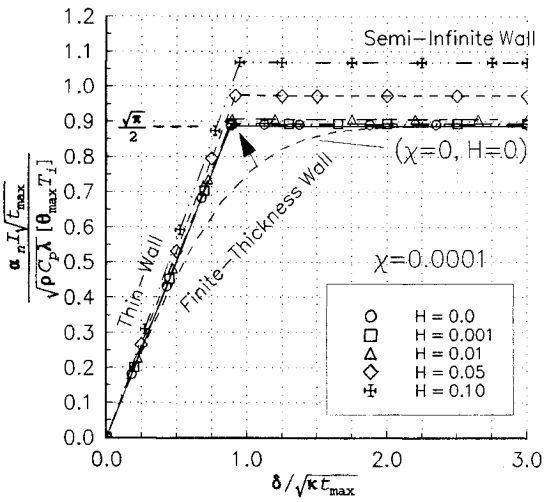

Fig. 2 Aluminum thermal absorption performance, $\chi = 0.0001$.

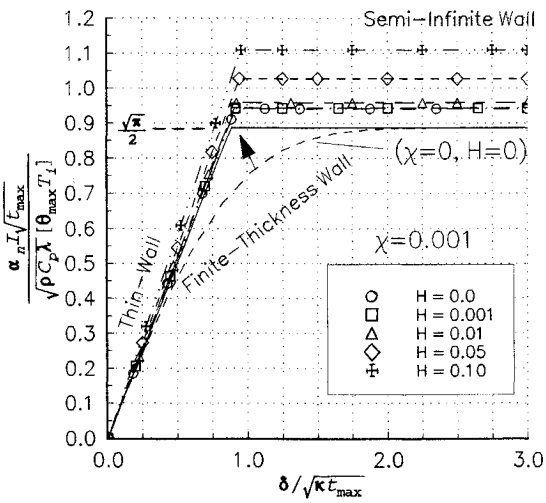

Fig. 3 Aluminum thermal absorption performance, $\chi = 0.001$.

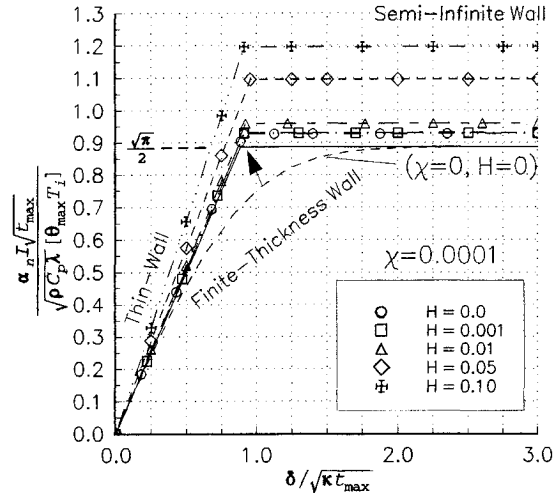

Fig. 4 Beryllium thermal absorption performance, $\chi = 0.0001$.

Comparing Figs. 2 and 4 illustrates and quantifies the increased enhancement in beryllium thermal absorption capability relative to aluminum for common χ and H. Higher thin wall performance (i.e., higher slope), and higher semi-infinite wall performance, of beryllium compared to aluminum reflects its higher thermal absorption capability. Beryllium not only has a higher θ_{max} than aluminum, but its higher temperature capability produces an additional advantage compared to aluminum from higher thermal radiative and convective cooling at the increased temperatures achievable during heat-up.

Each material has different sets of curves (like Figs. 2–4) because of different θ_{max}, and the fact that the reradiation/convection solutions are no longer linear in the nondimensional parameters, ψ_1 and ψ_2. When there is no surface reradiation or convection, the solutions are linear in the nondimensional parameters and the slope of θ vs ψ_n is constant. Materials with higher θ_{max} (i.e., higher temperature capability) gain a survivability benefit (i.e., longer exposure time) due only to the linear absorption effect. Consequently, all material thermal absorption performance curves then collapse into one curve for $\chi = 0$, $H = 0$. However, with surface reradiation and convection effects included, the nonlinear thermal response solutions have continuously decreasing θ vs ψ_n slopes due to significant reradiative and convective cooling effects. Thus, materials with higher θ_{max} (e.g., beryllium) gain an added survivability benefit (i.e., additionally longer exposure time) over and above the simple linear absorption effect. Therefore, what is one nondimensional curve in Rohsenow et al.[3] expands into a different set of nondimensional curves for each material with different θ_{max} (as in Figs. 2 and 4). Higher θ_{max} necessarily results in higher reradiative and convective cooling capability. The ultimate magnitude of thermal reradiation and convection effects is therefore material-dependent because of thermal response nonlinearities, and must be evaluated separately for different materials. It is not possible to draw general conclusions about the importance or unimportance of thermal reradiation/convection effects during constant-heat-flux irradiation for a broad range of materials. Figures 2–4 demonstrate that, for certain combinations of thermal radiation and convection parameters, the thermal reradiation and convection effects have a significant impact on material thermal response and survivability to constant-heat-flux irradiation.

This work demonstrates that first-order reradiative/convective cooling effects on material survivability, and resulting

exposure time enhancement and material thickness reduction, are uniquely and completely quantified by the nondimensional parameters; χ, H, and ψ_1 in thin-wall thermal response, and χ, H, and ψ_2 in semi-infinite and finite-wall thermal response. Maximum exposure times and minimum material thickness for various incident irradiation, thermal reradiation, and thermal convection conditions can be determined directly from these nondimensional parameters and thermal response solutions discussed above. Radiative and convective cooling effects are material-dependent and not necessarily negligible for some radiative and convective conditions.

References

[1]Carslaw, H. S., and Jaeger, J. C., *Conduction of Heat in Solids*, 2nd ed., Clarendon Press, Oxford, England, UK, 1959.

[2]Incropera, F. P., and De Witt, D. P., *Fundamentals of Heat and Mass Transfer*, 3rd ed., Wiley, New York, 1990.

[3]Rohsenow, W. M., and Hartnett, J. P. (eds.), *Handbook of Heat Transfer*, Sec. 3, McGraw-Hill, New York, 1973.

[4]Schriempf, J. T., "Response of Materials to Laser Radiation: A Short Course," Naval Research Lab. Rept. 7728, Washington, DC, 1974.

[5]Abarbanel, S. S., "Time Dependent Temperature Distribution in Radiating Solids," *Journal of Mathematics and Physics*, Vol. 39, No. 4, 1960, pp. 246–257.

[6]Bartholomeusz, B. J., "Thermal Response of a Laser-Irradiated Metal Slab," *Journal of Applied Physics*, Vol. 64, No. 8, 1988, pp. 3815–3819.

[7]Chen, H. T., and Chen, C. K., "Hybrid Laplace Transform/Finite-Element Method for Two-Dimensional Transient Heat Conduction," *Journal of Thermophysics and Heat Transfer*, Vol. 2, No. 1, 1988, pp. 31–36.

[8]Roy, S., and Modest, M. F., "Three-Dimensional Effects During Scribing with a CW Laser," *Journal of Thermophysics and Heat Transfer*, Vol. 4, No. 2, 1990, pp. 199–203.

[9]Modest, M. F., and Abakians, H., "Heat Conduction in a Moving Semi-Infinite Solid Subjected to Pulsed Laser Irradiation," *Journal of Heat Transfer*, Vol. 108, No. 3, 1986, pp. 597–601.

[10]Modest, M. F., and Abakians, H., "Evaporative Cutting of a Semi-Infinite Body with a Moving CW Laser," *Journal of Heat Transfer*, Vol. 108, No.3, 1986, pp. 602–607.

[11]Yuen, W. W., Khatami, M., and Cunnington, G. R., Jr., "Transient Radiative Heating of an Absorbing, Emitting, and Scattering Material," *Journal of Thermophysics and Heat Transfer*, Vol. 4, No. 2, 1990, pp. 193–198.

[12]Knight, C. J., "Transient Vaporization from a Surface into Vacuum," AIAA Paper 81-1274R, June 1981.

[13]Hendricks, T. J., "Perturbation Technique for Laser-Induced Thermal Response with Thermal Radiation Boundary Conditions," AIAA Paper 90-1680, June 1990.

Temperature and Heat Transfer Solutions for Aeromagnetic Dusty-Gas Flow

Ali J. Chamkha*

Fleetguard, Inc., Cookeville, Tennessee 38502

Introduction

TWO-PHASE (particle-fluid) suspensions occur in many industrial processes. Understanding such processes requires the analysis of the basic equations governing multiphase flows. These equations are given by Soo[1] and Marble.[2] Rossow[3] reported equations governing the flow of an electrically conducting fluid in the presence of a magnetic field. Aeromagnetic dusty-gas flows are of interest because they have many applications in the geophysical and astronomical sciences.

In a previous paper, Chamkha[4] reported exact solutions for hydromagnetic (or more correctly aeromagnetic) flow of a particulate suspension past an infinite porous plate. In his work, Chamkha[4] did not consider the thermal energy transport equations of the suspension. The purpose of this article is to study the effect of a transverse magnetic field on the temperature profiles, and the wall heat transfer for flow of a dusty gas past an infinite porous flat plate. The fluid phase is assumed to be incompressible and electrically conducting, and the particle phase is assumed to be incompressible and electrically nonconducting. The volume fraction of suspended particles is assumed to be small. It is also assumed that there is no radiative heat transfer from one particle to another and that the particles do not interact with each other.

Governing Equations

Consider steady laminar particle-fluid flow past an infinite porous flat plate. The flow is a uniform stream parallel to the x, y plane with the plate being coincident with the plane $y = 0$. Far from the plate, both phases are in equilibrium moving with a velocity V_∞ and a temperature T_∞ in the x direction. Let uniform fluid-phase suction with velocity V_0 be imposed at the plate surface. Since the plate is infinite, the physical variables will only depend on y (the distance above the plate).

In the present problem, it is assumed following Gupta[5] that no applied voltages exit. This corresponds to the case where no energy is being added or extracted from the fluid by electrical means. The magnetic effects are confined to retarding the flow and dissipating kinetic energy into internal energy. In general, the electrical current flowing in the fluid gives rise to an induced magnetic field that distorts the applied magnetic field. This would exist if the fluid were an electrical insulator. However, since the viscous boundary layer is thin, the induced magnetic field will be neglected compared to the constant applied field acting along the y axis and moving past the plate with the freestream velocity.

The governing equations for the problem under investigation are based on the balance laws of mass, linear momentum, and energy for both phases. These can be written in dimensional form, taking into account the assumptions mentioned earlier, as

$$-\rho V_0 u' = \mu u'' + \rho_p(u_p - u)/\tau_v - \sigma B_0^2(u - V_\infty) \quad (1)$$

$$-\rho_p V_0 u_p' = -\rho_p(u_p - u)/\tau_V \quad (2)$$

$$-\rho c V_0 T' = kT'' + \mu(u')^2 + c_p\rho_p(T_p - T)/\tau_T + \rho_p(u_p - u)^2/\tau_V + \sigma B_0^2(u - V_\infty)^2 \quad (3)$$

$$-\rho_p c_p V_0 T_p' = -\rho_p c_p(T_p - T)/\tau_T \quad (4)$$

where u is the fluid-phase velocity in the x direction, u_p is the particle-phase velocity in the x direction, ρ is the fluid-phase density, ρ_p is the particle-phase density, μ is the fluid-phase dynamic viscosity, V_0 is the suction velocity, σ is the electrical conductivity, B_0 is the magnetic induction, T is the fluid-phase temperature, T_p is the particle-phase temperature, k is the fluid-phase thermal conductivity, c is the fluid-phase specific heat at constant pressure, c_p is the particle-phase specific heat, τ_v and τ_T are the velocity relaxation time and the temperature relaxation time, respectively, and a prime denotes ordinary differentiation with respect to y. The minus signs appearing on the left side of Eqs. (1–4) result from the fact that the suction velocity is acting downward in the opposite direction of the positive y direction.

The last terms appearing in Eqs. (1) and (4) are present due to the presence of the magnetic field. The former rep-

Received April 30, 1992; revision received Aug. 6, 1992; accepted for publication Aug. 7, 1992. Copyright © 1992 by the American Institute of Aeronautics and Astronautics, Inc. All rights reserved.

*Staff Research Engineer, 1200 Fleetguard Road. Member AIAA.